

Logarithmic entanglement scaling in dissipative free-fermion systems

Antonio D'Abbruzzo,¹ Vincenzo Alba,² and Davide Rossini²

¹*Scuola Normale Superiore, I-56126 Pisa, Italy*

²*Dipartimento di Fisica dell'Università di Pisa and INFN, Sezione di Pisa, I-56127 Pisa, Italy*

(Dated: September 26, 2022)

We study the quantum information spreading in one-dimensional free-fermion systems in the presence of localized thermal baths. We employ a *nonlocal* Lindblad master equation to describe the system-bath interaction, in the sense that the Lindblad operators are written in terms of the Bogoliubov operators of the closed system, and hence are nonlocal in space. The statistical ensemble describing the steady state is written in terms of a convex combination of the Fermi-Dirac distributions of the baths. Due to the singularity of the free-fermion dispersion, the steady-state mutual information exhibits singularities as a function of the system parameters, akin to dynamical quantum phase transitions. While the mutual information generically satisfies an area law, at the singular points it exhibits logarithmic scaling as a function of subsystem size. By employing the generalized Fisher-Hartwig theorem, we derive the prefactor of the logarithmic scaling, which depends on the parameters of the baths and plays the role of an effective “central charge”. This is upper bounded by the central charge governing ground-state entanglement scaling. We provide numerical checks of our results in the paradigmatic tight-binding chain and the Kitaev chain.

I. INTRODUCTION

The study of the interplay between the microscopic quantum world and the macroscopic classical one is a fundamental research topic in contemporary physics, although it dates back to the first days of quantum mechanics [1, 2]. Typically, the interaction with the environment is believed to destroy genuine quantum behaviors, although consensus is emerging that this is not always the case. Dissipation-based protocols have been devised to imprint nontrivial correlations in quantum many-body systems (see, e.g., Refs. [3–12]). A first crucial question is whether entanglement, which is the distinctive feature of quantum mechanics, is robust against the presence of the environment. Second, is it possible to enhance the entanglement content of a quantum many-body state via an *ad hoc* engineered environment? Answering these questions is a daunting task, because there is no universal approach (neither analytic nor numerical) to tackle generic *open* quantum many-body systems. With this state of affairs, one has to resort to approximate treatments. Markovian master equations, such as the Lindblad master equation [13–15], provide some of the most successful tools to attack open quantum many-body systems.

In this paper we focus on the paradigmatic one-dimensional setup illustrated in Fig. 1: a system of *non-interacting* fermions is locally coupled to ideal thermal baths. To be specific, we focus on the tight-binding chain and on the Kitaev chain. The fermions live on a lattice with N sites, with either periodic boundary conditions (PBC) or open boundary conditions (OBC). The system is put in contact with two ideal fermionic reservoirs at temperatures T_L, T_R , and with chemical potentials μ_L, μ_R . With OBC the two baths are placed at the edges of the chain [Fig. 1 (a)], whereas with PBC they are at the maximum distance $N/2$ [Fig. 1 (b)]. The interaction between the chain and the reservoirs is treated within the formalism of the Lindblad master

equation [15]. Specifically, we employ the *nonlocal* description derived in Ref. [16]. The Lindblad operators are obtained *ab initio* from the microscopic system-bath interaction, and are written in terms of the Bogoliubov modes of the model without dissipation. As such, the Lindblad operators are non-local in real space. Interestingly, this allows to recover the Conformal Field Theory (CFT) description of the chain in the low-temperature limit. Furthermore, the nonlocal Lindblad approach allows to obtain a thermodynamically consistent description of transport properties [16, 17].

We are interested in the quantum correlations emerging in the steady state of finite chains of length N , in the limit $t \rightarrow \infty$. The ensemble describing this state is written in terms of a convex combination of the Fermi-Dirac distributions of the reservoirs [16]. Importantly, this ensemble is in general different from the finite-temperature ensemble of the underlying fermionic chain. In particular, we will show that ground-state criticality of the free chain Hamiltonian is associated with nontrivial steady-state correlations in the dissipative model. To monitor these correlations, we consider the quantum mutual information $I(A_1 : A_2)$ between two subregions A_1 and A_2 of the chain, defined as [18–21]

$$I(A_1 : A_2) := S_{A_1} + S_{A_2} - S_{A_1 \cup A_2}, \quad (1)$$

where S_A is the von Neumann entropy of the subregion A , which is defined as

$$S_A := -\text{Tr}(\rho_A \ln \rho_A), \quad (2)$$

where ρ_A is the reduced density matrix for subsystem A .

For pure states the von Neumann entropy S_A of a subsystem quantifies its entanglement with the rest of the system. Moreover, one has that $S_A = S_{\bar{A}}$, with \bar{A} being the complement of A [see, for instance, Fig. 1 (a)], and $S_{A \cup \bar{A}} = 0$. However, in the presence of an environment, the global state is mixed, which implies that neither the

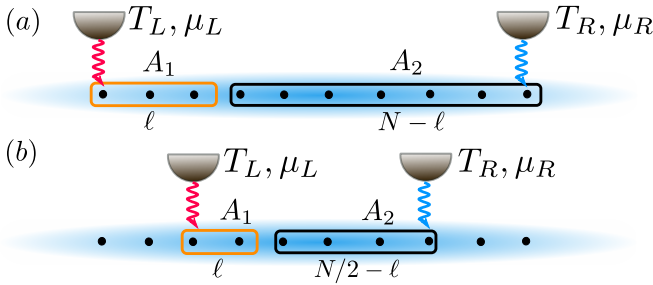


Figure 1. The setup used in this work. A one-dimensional chain of N noninteracting fermions is put in contact with two thermal reservoirs at temperatures T_L, T_R and chemical potentials μ_L, μ_R . (a) In the case of OBC, only the sites at the edges are in contact with the baths, and we are interested in the steady-state mutual information $I(A_1 : A_2)$ between the two connected intervals A_1 and A_2 of length ℓ and $N - \ell$, respectively. (b) In the case of PBC, the sites in contact with the baths are at the maximum distance $N/2$ and the intervals A_1 and A_2 are respectively of length ℓ and $N/2 - \ell$. Analytical calculations are done in the thermodynamic limit $N, \ell \rightarrow \infty$.

von Neumann entropy nor the mutual information are proper measures of the entanglement shared between different regions. Still, it has been shown recently that for out-of-equilibrium free-fermion and free-boson models in the presence of quadratic global dissipation the mutual information admits a hydrodynamic description in terms of a quasiparticle picture [22–25]. Moreover, we numerically checked that our findings remain qualitatively valid using the fermionic entanglement negativity, which instead is a proper measure of entanglement [26].

Both the full-system entropy, as well as the subsystems entropies, generally exhibit volume-law scaling in the steady-state. However, if the bulk of the system is tuned to a critical point, logarithmic corrections appear. Specifically we show that, for a generic subsystem A of length ℓ , in the scaling limit $N, \ell \rightarrow \infty$ with arbitrary ratio ℓ/N , the entropy S_A is given as

$$S_A = \alpha\ell + \frac{c(\Theta)}{3\nu} \ln \left[\frac{N}{\pi} \sin \left(\frac{\pi\ell}{N} \right) \right] + \mathcal{O}(1). \quad (3)$$

The prefactor α of the volume-law term depends on the full spectrum of the model and on the properties of the bath. A similar volume-law scaling has been found in free-fermion systems with localized dissipative impurities [27, 28]. The prefactor $c(\Theta)$ is an effective “central charge”, which contains information only about the singularities in the single-particle spectrum of the model. It is an even function of a parameter $\Theta \in [-1, 1]$ which depends on the properties of the baths, i.e., their temperatures and chemical potentials. The quantity $\nu \in \{1, 2\}$ is the number of boundary points between subsystem A and the rest. For instance, for a chain with OBC [see Fig. 1 (a)], $\nu = 2$ if the subsystem is next to the chain edge, whereas $\nu = 1$ if it is in the bulk. The argument inside the square brackets is the so-called chord length [29]. In the limit $\ell/N \rightarrow 0$, the second term in (3) becomes

$c/(3\nu) \ln(\ell)$, which we prove analytically. On the other hand, the result for finite ratio ℓ/N is a conjecture inspired by the zero-temperature CFT scaling [19]. Similar logarithmic terms as in (3) have been found in a tight-binding model, although for different nonequilibrium settings [30–33]. Finally, the last term $\mathcal{O}(1)$ is a subleading constant, which can be calculated, at least for the tight-binding chain, by using the Fisher-Hartwig conjecture [34–39].

In the limit $|\Theta| \rightarrow 1$ one recovers the zero-temperature result, i.e., $c(\Theta)$ becomes the central charge of the CFT that describes ground-state properties of the model. Here one has $c = 1$ and $c = 1/2$ for the tight-binding chain and the Kitaev chain, respectively. On the other hand, for $\Theta \rightarrow 0$, which corresponds to the high-temperature limit, $c(\Theta)$ vanishes. Remarkably, for generic Θ , the effective central charge of the tight-binding chain is twice that of the Kitaev model. Moreover, we show that $c(\Theta)$ is always upper bounded by the zero-temperature central charge of the models. Upon substituting the asymptotic scaling (3) in (1), one obtains that the volume-law term cancels out, and the mutual information exhibits logarithmic scaling.

The structure of the paper is as follows. In Sec. II we introduce the fermionic models we are interested in. In particular, Sec. II A 3 contains the calculation of the Majorana correlation matrix, which is important to determine entanglement properties, while the main formulas to determine the von Neumann entropies in terms of correlation functions are reviewed in Sec. II B. In Sec. III we summarize the treatment of thermal environments within the nonlocal Lindblad equation, which was derived in Ref. [16]; the main result is formula (51). In Sec. IV and Sec. V we derive Eq. (3) for the tight-binding chain and for the Kitaev chain, respectively. We provide numerical benchmarks of our results in Sec. VI: in particular, in Sec. VI A we overview the volume-law scaling of the von Neumann entropy, while in section VI B we discuss the scaling of the mutual information. Our conclusions are drawn in Sec. VII.

II. MODELS & METHODS

In this section we describe the basic framework used in this work. We first introduce the quadratic fermionic Hamiltonians of interest, in Sec. II A. Then we review the tight-binding chain (Sec. II A 1) and the Kitaev chain (Sec. II A 2). In Sec. II A 3 we provide some general formulas for the two-point correlation of Majorana operators in the two models. These are essential to study entanglement properties. In Sec. II B we summarize the calculation of the von Neumann entropy via correlation matrix techniques [40]. In Sec. III we review the approach of Ref. [16] to derive a *nonlocal* Lindblad description of fermionic chains in contact with localized thermal baths.

A. Fermionic quadratic Hamiltonians

We focus on free-fermion chains [41, 42]. Let \mathcal{S} be a quantum system on a lattice with N sites and $H_{\mathcal{S}}$ its second-quantized Hamiltonian, which can be written in terms of fermionic raising and lowering operators a_n^\dagger, a_n , with $n \in \{1, \dots, N\}$. We assume $H_{\mathcal{S}}$ to be quadratic, i.e.,

$$H_{\mathcal{S}} = \sum_{n,m=1}^N \left[Q_{nm} a_n^\dagger a_m + \frac{P_{nm}}{2} (a_n^\dagger a_m^\dagger - a_n a_m) \right], \quad (4)$$

with Q, P being $N \times N$ real matrices satisfying $Q^T = Q$ and $P^T = -P$. It is known that $\mathcal{H}_{\mathcal{S}}$ can be written in diagonal form as

$$H_{\mathcal{S}} = E_0 + \sum_k \omega_k b_k^\dagger b_k, \quad (5)$$

where $\omega_k \geq 0$ is the single-particle dispersion, E_0 is an irrelevant constant, b_k^\dagger, b_k are new fermionic operators (the Bogoliubov modes), and the index k denotes the quasimomentum. The operators b_k are written as linear superpositions of the original fermions. Specifically, one has

$$b_k := \sum_{n=1}^N (X_{kn} a_n + Y_{kn} a_n^\dagger), \quad (6)$$

where X and Y are appropriately chosen $N \times N$ complex matrices. For the following it is useful to define the so-called Lieb-Schultz-Mattis matrices [41] ϕ, ψ as

$$\phi := (X + Y)^\dagger, \quad \psi := (X - Y)^\dagger. \quad (7)$$

In general, these are complex $N \times N$ matrices that encode information about the Majorana correlation functions of the model (see Sec. II A 3).

1. Tight-binding chain

The tight-binding chain model is obtained from (4) by fixing

$$Q_{nm} = -J\delta_{n,m-1} - J\delta_{n,m+1} - h\delta_{nm}, \quad P_{nm} = 0, \quad (8)$$

where h is an external magnetic field strength, and J is the hopping amplitude between nearest-neighbor sites. Thus, the Hamiltonian reads as

$$H_{\mathcal{S}} = -J \sum_{n=1}^N (a_n^\dagger a_{n+1} + a_{n+1}^\dagger a_n) - h \sum_{n=1}^N a_n^\dagger a_n, \quad (9)$$

where a_{N+1} is determined by the boundary conditions: with OBC we are choosing $a_{N+1} = 0$, whereas with PBC we have $a_{N+1} = a_1$.

The single-particle dispersion relation [cf. Eq. (5)] is given by [43]

$$\omega_k = |h + 2 \cos(k)|, \quad (10)$$

where $(n = 1, \dots, N)$:

$$k = \begin{cases} n\pi/(N+1) & \text{(for OBC),} \\ 2\pi n/N & \text{(for PBC).} \end{cases} \quad (11)$$

The functions ϕ_{nk} and ψ_{nk} [cf. Eqs. (7)] are given by

$$\phi_{nk} = \begin{cases} \sqrt{2/(N+1)} \sin(kn) & \text{(for OBC),} \\ e^{ikn}/\sqrt{N} & \text{(for PBC),} \end{cases} \quad (12a)$$

$$\psi_{nk} = \text{sgn}(-h - 2 \cos(k)) \phi_{nk}, \quad (12b)$$

where $\text{sgn}(x)$ is the sign function and the corresponding quasimomentum index has to be chosen as in (11). The ground state of the tight-binding model is annihilated by all the Bogoliubov operators b_k [cf. Eq. (6)], and it exhibits criticality for $|h| \leq 2$. For $|h| < 2$, its properties are described by a CFT [29] with central charge $c = 1$.

The entanglement properties of free-fermion systems are encoded in the fermionic two-point correlation functions [44]. Let us first discuss the open tight-binding chain. In the limit $N \rightarrow \infty$, the ground-state fermionic correlation function $C_{nm}^{(\text{obc})} := \langle a_n^\dagger a_m \rangle$ is given as [44]

$$C_{nm}^{(\text{obc})} = \int_{-\pi}^{\pi} \frac{dk}{2\pi} \Theta_H(k_F - |k|) [e^{ik(n-m)} - e^{ik(n+m)}], \quad (13)$$

where $\Theta_H(\cdot)$ is the Heaviside step function, $n, m \in [1, \infty)$, and k_F is the Fermi momentum

$$k_F := \arccos\left(-\frac{h}{2}\right). \quad (14)$$

Performing the integral in (13), one obtains

$$C_{nm}^{(\text{obc})} = \frac{\sin(k_F(n-m))}{\pi(n-m)} - \frac{\sin(k_F(n+m))}{\pi(n+m)}. \quad (15)$$

The result for the periodic infinite chain can be recovered from (15) by taking the limit $n, m \rightarrow \infty$ with $n-m$ fixed, i.e., by considering correlators in the bulk of the open chain. Thus, only the first term in (13) survives and one obtains

$$C_{nm}^{(\text{pbc})} = \frac{\sin(k_F(n-m))}{\pi(n-m)}. \quad (16)$$

It is useful to observe that the first term in (13) depends only on the difference $n-m$, reflecting translation invariance, and it defines a so-called Toeplitz matrix [38], with symbol $\Theta_H(k_F - |k|)$. The second term in (13) depends only on $n+m$, which defines a so-called Hankel matrix. Thus, the full correlator exhibits a Toeplitz-plus-Hankel structure.

Crucially, for $|h| > 2$ the symbol of the correlator in (13) is smooth as a function of k . On the other hand,

for $|h| < 2$ it exhibits a jump discontinuity at $\pm k_F$, which is the main signature of critical behavior. This non analytic behavior gives rise to a logarithmic violations of the area law in the ground-state entanglement entropies [19, 21]. In the following sections, by using the approach of Ref. [16] we will show that in the presence of thermal baths locally coupled to the chain, the steady-state fermionic correlator exhibits a similar structure as in Eq. (13). In particular, even though the symbol of the correlator is affected by the presence of the bath, it is not smooth as a function of k . This gives rise to logarithmic scaling of the steady-state mutual information.

2. Kitaev chain

Let us now consider the Kitaev chain [45]. This is obtained from (4) by choosing

$$Q_{nm} = -J\delta_{n,m-1} - J\delta_{n,m+1} - h\delta_{n,m}, \quad (17a)$$

$$P_{nm} = -\Delta\delta_{n,m-1} + \Delta\delta_{n,m+1}, \quad (17b)$$

with J the hopping strength, h a magnetic field, and Δ the strength of the pairing term. In the following, we will set $\Delta = J = 1$. Thus, the Hamiltonian of the Kitaev chain reads as

$$H_S = -\sum_{n=1}^N \left(a_n^\dagger a_{n+1} + a_n^\dagger a_{n+1}^\dagger + \text{h.c.} \right) - h \sum_{n=1}^N a_n^\dagger a_n. \quad (18)$$

For this model we exclusively employ PBC, choosing $a_{N+1} = a_1$, and we assume $h \neq 0$. The Hamiltonian (18) can be rewritten as in (5) with single-particle dispersion

$$\omega_k = \sqrt{h^2 + 4h \cos(k) + 4}, \quad (19)$$

where the index k is chosen as in (11) for PBC. The functions ϕ_{jk} and ψ_{jk} [cf. Eqs. (7)] that encode the Fourier transform and the Bogoliubov transformation needed to diagonalize (18) are given by

$$\phi_{jk} = \frac{e^{ikj}}{\sqrt{N}}, \quad (20a)$$

$$\psi_{jk} = e^{i\xi(k)} \phi_{jk}, \quad (20b)$$

where we defined

$$e^{i\xi(k)} := -\frac{h + 2e^{ik}}{\omega_k} \quad (21)$$

and the so-called Bogoliubov angle $\xi(k) \in \mathbb{R}$ is defined by

$$\cos \xi(k) = -\frac{h + 2 \cos k}{\sqrt{h^2 + 4h \cos k + 4}}, \quad (22a)$$

$$\sin \xi(k) = \frac{2 \sin k}{\sqrt{h^2 + 4h \cos k + 4}}. \quad (22b)$$

It is clear that $\xi(k)$ is continuous as a function of k , for $|h| \neq 2$. For $h = 2$, a jump discontinuity appears at

$k = \pm\pi$, while for $h = -2$ it emerges for $k = 0$. As for the tight-binding chain (see section II A 1), for $|h| = 2$ long-wavelength properties of the ground state of the Kitaev chain are described by a CFT with central charge $c = 1/2$. Consequently, the ground state exhibits logarithmic violations of the area law for the von Neumann entropies. Again, below we show that the singular structure of Eqs. (22) survives in the presence of localized baths, giving rise to logarithmic scaling of the mutual information.

3. Majorana correlation function

To determine entanglement-related quantities, it is convenient to introduce the Majorana operators [46, 47]:

$$w_{2n-1} = \frac{1}{\sqrt{2}} (a_n^\dagger + a_n), \quad w_{2n} = \frac{i}{\sqrt{2}} (a_n^\dagger - a_n). \quad (23)$$

It is straightforward to write these in terms of the Bogoliubov operators b_k that diagonalize the models [cf. (5)]:

$$\begin{bmatrix} w_{2n-1} \\ w_{2n} \end{bmatrix} = \frac{1}{\sqrt{2}} \sum_k \begin{bmatrix} \phi_{nk} & \phi_{nk}^* \\ -i\psi_{nk} & i\psi_{nk}^* \end{bmatrix} \begin{bmatrix} b_k \\ b_k^\dagger \end{bmatrix}, \quad (24)$$

where ϕ_{nk} and ψ_{nk} are given in Eqs. (7). For the tight-binding chain and the Kitaev chain ϕ_{nk}, ψ_{nk} are reported in Eqs. (12) and (20), respectively. One can show that the generic expectation value $\langle w_a w_b \rangle$ is written as

$$\langle w_a w_b \rangle = \frac{\delta_{ab} + i\Gamma_{ab}}{2}, \quad (25)$$

where Γ is a $2N \times 2N$ matrix of the form

$$\Gamma = \begin{bmatrix} \Pi_{11} & \Pi_{12} & \cdots & \Pi_{1N} \\ \Pi_{21} & \Pi_{22} & \cdots & \Pi_{2N} \\ \vdots & \vdots & \ddots & \vdots \\ \Pi_{N1} & \Pi_{N2} & \cdots & \Pi_{NN} \end{bmatrix}, \quad (26)$$

with Π_{nm} being a 2×2 block defined by

$$\Pi_{nm} := \begin{bmatrix} 0 & \text{Re}[\phi \theta \psi^\dagger]_{nm} \\ -\text{Re}[\phi \theta \psi^\dagger]_{mn} & 0 \end{bmatrix}. \quad (27)$$

In writing (27) we assumed the matrix $K_{kq} := \langle b_k^\dagger b_q \rangle$ to be diagonal and the matrix $F_{kq} := \langle b_k b_q \rangle$ to be zero, which will turn out to be true in our formalism (see Sec. III). Here θ_{kq} is the occupation of the Bogoliubov modes b_k given by

$$\theta_{kq} = \delta_{kq} (1 - 2\langle b_k^\dagger b_k \rangle). \quad (28)$$

Notice that Γ is a real skew-symmetric matrix of even dimension. This means that it has pairs of eigenvalues $\pm i\nu_r$ with $\nu_r \in \mathbb{R}$.

Let us now specialize the matrix Γ to the case of the tight-binding chain (see section II A 1). By using Eqs. (12) in (27) we obtain

$$G_{nm} := \text{Re}[\phi \theta \psi^\dagger]_{nm} = \delta_{nm} - 2 C_{nm}, \quad (29)$$

where $C_{nm} = \langle a_n^\dagger a_m \rangle$ is the fermion correlation function. This implies that

$$\Gamma = G \otimes \begin{bmatrix} 0 & 1 \\ -1 & 0 \end{bmatrix}, \quad (30)$$

from which we conclude that the eigenvalues of Γ are $\pm i\nu_r$ if and only if ν_r are the eigenvalues of G .

Let us now consider the Kitaev chain with PBC. By using Eqs. (20) we obtain

$$\text{Re}[\phi \theta \psi^\dagger]_{nm} = \frac{1}{N} \text{Re} \sum_k \theta_{kk} e^{-i\xi(k)} e^{ik(n-m)}, \quad (31)$$

where $\xi(k)$ is defined in (21), and θ_{kk} is given in (28). Using the fact that θ_{kk} is an even function of k and $\xi(k)$ is an odd one, we can write

$$\Pi_{nm} = \int_{-\pi}^{\pi} \frac{dk}{2\pi} \begin{bmatrix} 0 & \theta_{kk} e^{-i\xi(k)} \\ -\theta_{kk} e^{i\xi(k)} & 0 \end{bmatrix} e^{ik(n-m)}, \quad (32)$$

where we took the thermodynamic limit $N \rightarrow \infty$. Eq. (32) holds for a generic thermodynamic state, which is characterized by the functions θ_{kk} . Like for the tight-binding chain, the ground-state of the Kitaev chain is the vacuum state of all the Bogoliubov operators b_k . In this case $\theta_{kk} = 1$ [cf. (28)], and the ground-state is characterized by

$$\Pi_{nm}^{(\text{GS})} = \int_{-\pi}^{\pi} \frac{dk}{2\pi} \begin{bmatrix} 0 & e^{-i\xi(k)} \\ -e^{i\xi(k)} & 0 \end{bmatrix} e^{ik(n-m)}. \quad (33)$$

In the presence of external thermal baths, the Majorana correlator Γ is determined by (32), with θ_{kk} encoding the properties of the baths.

B. Entropy in free-fermion systems

For free-fermion systems, the von Neumann entropy (2) of a subsystem A of length ℓ (see Fig. 1), and the Rényi entropies in general [44], are obtained from the Majorana correlation matrix Γ_A , which is obtained from (26) by restricting $n, m \in A$. If $\pm i\nu_r$ are the eigenvalues of Γ_A , then

$$S_A = \sum_{r=1}^{\ell} e(1, \nu_r), \quad (34)$$

where we defined the function $e(x, \nu)$ as

$$e(x, \nu) := -\frac{x - \nu}{2} \ln\left(\frac{x - \nu}{2}\right) - \frac{x + \nu}{2} \ln\left(\frac{x + \nu}{2}\right). \quad (35)$$

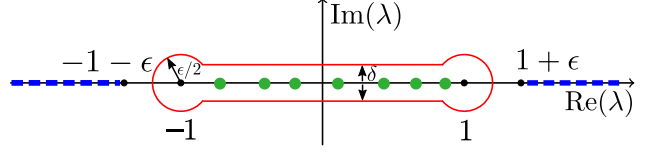


Figure 2. Contour γ in the complex plane for λ used to compute the von Neumann entropy of an interval [cf. Eq. (37)]. Dashed lines at $(-\infty, -1 - \epsilon] \cup [1 + \epsilon, \infty)$ denote a branch cut. Dots in the region $[-1, 1]$ are the zeros of $D_\ell(\lambda)$ [cf. Eq. (36)], or, equivalently, the poles of $dD_\ell(\lambda)/d\lambda$. Here we are interested in the limits $\epsilon \rightarrow 0$ and $\delta \rightarrow 0$.

Notice that Eq. (34) is well-defined because one can show that $-1 \leq \nu_r \leq 1$.

It is convenient to rewrite the sum in Eq. (34) as an integral in the complex plane. To this purpose we define the determinant

$$D_\ell(\lambda) := \det(\lambda \mathbb{1} - i\Gamma_A). \quad (36)$$

A straightforward application of Cauchy's theorem allows to rewrite Eq. (34) as

$$S_A = \lim_{\delta, \epsilon \rightarrow 0^+} \frac{1}{4\pi i} \oint_{\gamma} d\lambda e(1 + \epsilon, \lambda) \frac{d \ln D_\ell(\lambda)}{d\lambda}, \quad (37)$$

where we used the fact that $e(1, \nu) = e(1, -\nu)$. The contour γ in the complex plane is shown in Fig. 2. Dashed blue lines in the figure are the branch cuts of $e(1 + \epsilon, \lambda)$ at $(-\infty, -1 - \epsilon] \cup [1 + \epsilon, \infty)$. The horizontal parts of the contour are shifted by δ from the real axis. Finally, the function $d \ln(D_\ell)/d\lambda$ has simple poles in the interval $[-1, 1]$ (green dots in the figure). In the limit $\ell \rightarrow \infty$ the poles become dense, forming a new branch cut. The strategy [40] to obtain the asymptotic scaling of S_A in the limit $\ell = |A| \rightarrow \infty$ is to first obtain D_ℓ in the limit $\ell \rightarrow \infty$, then using it in Eq. (37).

III. GLOBAL LINDBLAD MASTER EQUATION

To make the paper self contained, we now recap the formalism used to treat self consistently thermal baths in the Lindblad approximation, within quadratic models [16]. Let us consider the interaction between the fermionic chain \mathcal{S} and the environment \mathcal{E} (see Fig. 1). The global system $\mathcal{U} = \mathcal{S} \cup \mathcal{E}$ is described by the Hamiltonian $H_{\mathcal{U}} = H_{\mathcal{S}} \otimes \mathbb{1}_{\mathcal{E}} + \mathbb{1}_{\mathcal{S}} \otimes H_{\mathcal{E}} + H_I$, where $H_{\mathcal{E}}$ is the Hamiltonian of the environment and H_I models the interaction between system and environment. We can always write H_I in the form

$$H_I = \sum_{\alpha} O_{\alpha} \otimes R_{\alpha}, \quad (38)$$

where O_{α} and R_{α} are Hermitian operators acting on \mathcal{S} and \mathcal{E} , respectively. In the following we restrict ourselves

to the situation in which O_α act nontrivially only on a finite number of sites of the chain (see Fig. 1).

Given a state $\rho(t)$ of the entire system $\mathcal{S} \cup \mathcal{E}$, we are interested in the evolution of the reduced density matrix $\rho_{\mathcal{S}}(t) := \text{Tr}_{\mathcal{E}}[\rho(t)]$. In the Markovian regime, the dynamics is described by a Lindblad master equation of the form [15]

$$\frac{d\rho_{\mathcal{S}}(t)}{dt} = -i[H, \rho_{\mathcal{S}}(t)] + \mathcal{D}(\rho_{\mathcal{S}}(t)), \quad (39)$$

where both H and \mathcal{D} have to be determined. Let us assume that the environment consists of a finite number of uncorrelated fermionic infinite thermal baths, such that

$$H_{\mathcal{E}} = \sum_{\alpha} \int dp \varepsilon_{\alpha,p} d_{\alpha,p}^\dagger d_{\alpha,p}, \quad (40)$$

where α is here an index that labels the bath, $d_{\alpha,p}$ the fermionic operators of the bath, and $\varepsilon_{\alpha,p}$ the bath dispersion. We also consider a generic linear coupling [cf. Eq. (38)] between the system and the baths:

$$O_{\alpha} = \sum_{j \in \mathcal{I}_{\alpha}} (a_j + a_j^\dagger), \quad (41)$$

$$R_{\alpha} = \int dp g_{\alpha,p} (d_{\alpha,p} + d_{\alpha,p}^\dagger), \quad (42)$$

where $g_{\alpha,p}$ is the strength of the coupling and \mathcal{I}_{α} are the sites of \mathcal{S} that are coupled to the bath α . Here we focus on the situation in which each bath is coupled to a single site of the system. For instance, for the case in Fig. 1 (a), one has $\alpha = 1, 2$ with $\mathcal{I}_1 = \{1\}$ and $\mathcal{I}_2 = \{N\}$.

The dissipator \mathcal{D} in Eq. (39) can be written as [16]

$$\mathcal{D}(\rho) = \sum_{\alpha,k} \gamma_{\alpha,k} \left[(1 - f_{\alpha}(\omega_k)) (2b_k \rho b_k^\dagger - \{b_k^\dagger b_k, \rho\}) + f_{\alpha}(\omega_k) (2b_k^\dagger \rho b_k - \{b_k b_k^\dagger, \rho\}) \right], \quad (43)$$

where we removed the subscript \mathcal{S} in $\rho_{\mathcal{S}}$, and where f_{α} is the Fermi-Dirac distribution associated with bath α ,

$$f_{\alpha}(\omega) = \frac{1}{1 + e^{\beta_{\alpha}(\omega - \mu_{\alpha})}}, \quad \beta_{\alpha} = \frac{1}{T_{\alpha}}. \quad (44)$$

Here T_{α}, μ_{α} are the temperature of the bath and chemical potential, respectively. In Eq. (43), b_k denote the Bogoliubov operators that diagonalize the system [cf. (6)], whereas ω_k are the single-particle energies [cf. (5)]. As is clear from Eq. (43), dissipation is encoded via the action of the Bogoliubov modes. The factors $f_{\alpha}(\omega_k)$ and $1 - f_{\alpha}(\omega_k)$ reflect the effect of the baths. Now, although the interaction Hamiltonian H_I is local in space, the dissipator $\mathcal{D}(\rho)$ is written in terms of Bogoliubov operators b_k , which are nonlocal. In contrast, with common approaches the Lindblad operators are chosen *ad hoc* and are typically local. Information about the locality of the baths is encoded in the functions $\gamma_{\alpha,k}$, defined as

$$\gamma_{\alpha,k} := J_{\alpha}(\omega_k) \left| \sum_{j \in \mathcal{I}_{\alpha}} \phi_{jk} \right|^2, \quad (45)$$

where ϕ_{jk} is given in Eq. (7) and $J_{\alpha}(\omega)$ is the spectral density of the bath,

$$J_{\alpha}(\omega) := \pi \int dp |g_{\alpha,p}|^2 \delta(\omega - \varepsilon_{\alpha,p}). \quad (46)$$

Besides the dissipative effect encoded in $\mathcal{D}(\rho)$, the presence of the baths also renormalizes the unitary part of the Lindblad equation (39). Indeed, the effective Hamiltonian H reads

$$H = \sum_k \tilde{\omega}_k b_k^\dagger b_k, \quad (47)$$

where the “dressed” single-particle dispersion $\tilde{\omega}_k$ reads

$$\tilde{\omega}_k = \omega_k \left(1 + \frac{2}{\pi} \sum_{\alpha} \left| \sum_{j \in \mathcal{I}_{\alpha}} \phi_{jk} \right|^2 \mathcal{P} \int_0^{\infty} d\epsilon \frac{J_{\alpha}(\epsilon)}{\omega_k^2 - \epsilon^2} \right), \quad (48)$$

with \mathcal{P} denoting Cauchy’s principal value.

Crucially, the Lindblad equation (39) is derived by using a *full secular approximation* [16, 17], which neglects rapidly oscillating terms $\propto \exp(i(\omega_k - \omega_{k'})t)$. Moreover, we neglect degeneracy in the spectrum, assuming that $\omega_k \neq \omega_{k'}$ if $k \neq k'$. Both these approximations are in general uncontrolled, and checking their validity would require an *ab initio* treatment of the baths.

The master equation (39) is quadratic in the Bogoliubov operators b_k, b_k^\dagger . This means that if the state of the system is Gaussian at a certain initial time, it will remain Gaussian at all times. Therefore, the state ρ is completely determined by the two-point functions of the Majorana fermions (23). Equivalently, one can use the correlators K_{kq} and F_{kq} defined as

$$K_{kq} := \text{Tr}(\rho b_k^\dagger b_q), \quad (49a)$$

$$F_{kq} := \text{Tr}(\rho b_k b_q). \quad (49b)$$

A direct computation allows to obtain the evolution of K_{kq} and F_{kq} as [16]

$$\begin{aligned} \frac{dK_{kq}}{dt} &= \left[i(\tilde{\omega}_k - \tilde{\omega}_q) \right. \\ &\quad \left. - \sum_{\alpha} (\gamma_{\alpha,k} + \gamma_{\alpha,q}) \right] C_{kq}(t) + 2\delta_{kq} \sum_{\alpha} \gamma_{\alpha,k} f_{\alpha}(\omega_k), \end{aligned} \quad (50a)$$

$$\frac{dF_{kq}}{dt} = \left[-i(\tilde{\omega}_k + \tilde{\omega}_q) - \sum_{\alpha} (\gamma_{\alpha,k} + \gamma_{\alpha,q}) \right] F_{kq}(t). \quad (50b)$$

Here $\tilde{\omega}_k$ are the modified single-particle energies in Eq. (48), the rates $\gamma_{\alpha,k}$ are defined in Eq. (45), and $f_{\alpha}(\omega)$ is the Fermi-Dirac distribution of the bath [cf. Eq. (44)]. We anticipate that, for the tight-binding chain and for the Kitaev chain, due to the simple structure of Eqs. (12) and (20), the dependence on $\gamma_{\alpha,k}$ drops out. Assuming that $\gamma_{\alpha,k}$ are not all equal to zero (which is obviously true

if the system is actually coupled to the environment), in the stationary limit $t \rightarrow \infty$ we obtain

$$K_{kq} = \delta_{kq} \frac{\sum_{\alpha} \gamma_{\alpha,k} f_{\alpha}(\omega_k)}{\sum_{\alpha} \gamma_{\alpha,k}}, \quad F_{kq} = 0. \quad (51)$$

Thus the correlation function in momentum space becomes diagonal, and it is a convex combination of the Fermi-Dirac distributions of the baths. Equation (51) is the main ingredient to extract steady-state properties of the system (see Sec. IV and Sec. V). Note that, if the baths are identical (f_{α} does not depend on α), we obtain $K_{kq} = \delta_{kq} f(\omega_k)$. Interestingly, even in this situation, the statistical ensemble that describes the steady state is not the standard finite-temperature ensemble of the underlying free-fermion model, due to the nonzero chemical potential in Eq. (44). As we will show in the following, this implies that the steady-state von Neumann entropy exhibits logarithmic additive corrections to the expected volume-law scaling at finite temperature.

IV. SCALING OF ENTROPY IN THE TIGHT-BINDING CHAIN

In this section we derive the scaling equation (3) of the steady-state von Neumann entropy for a subinterval of the tight-binding chain [cf. Eq. (9)]. A similar calculation was performed in [30, 31], but for a nonequilibrium setting which is different from ours.

First of all, using the definitions of ϕ_{nk} and ψ_{nk} reported in Eqs. (12), the steady-state fermionic correlation matrix G_{nm} of Eq. (29) for $N \rightarrow \infty$ reads

$$G_{nm} = \int_{-\pi}^{\pi} \frac{dk}{2\pi} \tilde{\theta}_{kk} \left[e^{ik(n-m)} - \zeta e^{ik(n+m)} \right], \quad (52)$$

where $\zeta = 0$ and $\zeta = 1$ corresponds to PBC and OBC, respectively. This equation defines a Toeplitz matrix for $\zeta = 0$, whereas one has a Toeplitz-plus-Hankel matrix [38] for $\zeta = 1$. The so-called symbol of G_{nm} is

$$\tilde{\theta}_{kk} := \theta_{kk} \operatorname{sgn}(-h - 2\cos(k)), \quad (53)$$

where θ_{kk} is given in Eq. (28) and the sign function is the same as in Eq. (12b). The function θ_{kk} encodes the information about the steady state and is obtained from (51). For now we consider generic θ_{kk} , specializing to the situations described in Fig. 1 (a) and (b), in Sec. IV A and IV B respectively. The function $\tilde{\theta}_{kk}$ is smooth, except for the sign function which displays a singularity for $|h| < 2$, thus giving rise to logarithmic corrections to the von Neumann entropy.

To extract the scaling behavior of the mutual information (1) one has to determine the asymptotic scaling of the von Neumann entropy S_A for a subsystem A of length $\ell \rightarrow \infty$. To that purpose, we first study the asymptotic behavior of $D_{\ell}(\lambda) \equiv D_{\ell}[g_{\lambda}]$ in Eq. (36), being the determinant of the Toeplitz (or Toeplitz-plus-Hankel) matrix

with symbol $g_{\lambda}(k) := \lambda - \tilde{\theta}_{kk}$ given by

$$g_{\lambda}(k) = \begin{cases} \lambda - \theta_{kk} & k \in [-\pi, -k_F] \cup [k_F, \pi], \\ \lambda + \theta_{kk} & k \in [-k_F, k_F]. \end{cases} \quad (54)$$

1. Periodic boundary conditions

Let us first consider the case of PBC [$\zeta = 0$ in Eq. (52)]. From that equation we obtain

$$\lambda \delta_{nm} - G_{nm} = \int_{-\pi}^{\pi} \frac{dk}{2\pi} e^{ik(n-m)} g_{\lambda}(k). \quad (55)$$

We now apply a specialized version of the Fisher-Hartwig conjecture [34] [48] in which the symbol $g_{\lambda}(k)$ is allowed to have only jump discontinuities at a finite number of points k_r . To apply it one has to rewrite $g_{\lambda}(k)$ in the form

$$g_{\lambda}(k) = g_s(k) \prod_{r=1}^R e^{ib_r(k-k_r-\pi \operatorname{sgn}(k-k_r))}. \quad (56)$$

Here $g_s(k)$ is a smooth function of k , R is the number of discontinuities of the symbol, and b_r, k_r are real constants. The Fisher-Hartwig conjecture states that, in the limit $\ell \rightarrow \infty$, one has

$$D_{\ell}[g_{\lambda}] \sim F[g_s]^{\ell} \left(\prod_{j=1}^R \ell^{-b_j^2} \right) E[g_{\lambda}], \quad (57)$$

where we defined

$$F[g_s] := \exp \left(\int_{-\pi}^{\pi} \frac{dk}{2\pi} \ln g_s(k) \right). \quad (58)$$

From Eq. (37) it is clear that the first factor in (57) gives a volume-law von Neumann entropy, and it is not sensitive to the singularities in the symbol $g_{\lambda}(k)$. The second factor is responsible for the logarithmic scaling of the von Neumann entropy and contains information about the singularities of $g_{\lambda}(k)$. The constant E is a known function of $g_{\lambda}(k)$. In the following, we are not considering E because we are interested only in the linear growth of the von Neumann entropy and in the logarithmic correction. The Fisher-Hartwig conjecture has been employed in the literature to determine the scaling behavior of the von Neumann and Rényi entropies in the ground state of critical fermionic chains [39, 40, 49].

It is straightforward to check that in our case the symbol $g_{\lambda}(k)$ in (54) can be written in the form (56) with two discontinuities at $k_1 = -k_F$ and $k_2 = k_F$, i.e., with $R = 2$, and

$$b_1 = -b_2 = \beta_{\lambda} + m, \quad (59)$$

where m is an integer and

$$\beta_{\lambda} = \frac{1}{2\pi i} \ln \left(\frac{\lambda - \Theta}{\lambda + \Theta} \right), \quad \text{with } \Theta := \theta_{kk}|_{k=k_F}. \quad (60)$$

Importantly, the parameter Θ for the tight-binding chain is the steady-state density of Bogoliubov excitations at the Fermi level, which contains information about the environment. We anticipate that Θ fully determines the logarithmic scaling of the von Neumann entropy. The function $g_s(k)$ is given by

$$g_s(k) = \left(\frac{\lambda + \Theta}{\lambda - \Theta} \right)^{\frac{k_F}{\pi} - 1} (\lambda + \theta_{kk}) \Theta_H(k_F - |k|) + \left(\frac{\lambda + \Theta}{\lambda - \Theta} \right)^{\frac{k_F}{\pi}} (\lambda - \theta_{kk}) \Theta_H(|k| - k_F). \quad (61)$$

Notice that $g_s(k)$ is not smooth as a function of k because it has a cusp-like singularity at $k = \pm k_F$. However, this is not expected to affect the logarithmic subleading term in the von Neumann entropy, as we are going to verify numerically in section VI. Now, upon substituting (59) (60) (61) in (57), we obtain that the von Neumann entropy of an interval A of length ℓ embedded in an infinite chain, in the limit $\ell \rightarrow \infty$ is given by

$$S_A = \alpha \ell + \frac{c(\Theta)}{3} \ln(\ell) + \mathcal{O}(1). \quad (62)$$

Here $c(\Theta)$, with Θ defined in (60), originates from the term in the round brackets in (57) and will be determined below. The constant α in (62) is determined by the first term in (57). By using (37) one obtains

$$\alpha = \lim_{\delta, \epsilon \rightarrow 0^+} \frac{1}{4\pi^2 i} \oint_{\gamma} d\lambda \int_{-\pi}^{\pi} dk \frac{e(1 + \epsilon, \lambda)}{\lambda + \text{sgn}(k_F - |k|) \theta_{kk}}, \quad (63)$$

where $e(x, \nu)$ is defined in (35), θ_{kk} in (28), and γ denotes the contour shown in Fig. 2. Performing such integral with the residue theorem, we get

$$\begin{aligned} \alpha &= \int_{-\pi}^{\pi} \frac{dk}{2\pi} e(1, \theta_{kk}), \\ &= - \int_{-\pi}^{\pi} \frac{dk}{2\pi} [K_{kk} \ln(K_{kk}) + (1 - K_{kk}) \ln(1 - K_{kk})], \end{aligned} \quad (64)$$

K_{kk} being the steady-state correlation function given in Eq. (51). Equation (64) is the steady-state density (i.e., the von Neumann entropy per volume) of the full system in the $N \rightarrow \infty$ limit. Specifically, we have that

$$\alpha = \lim_{\ell \rightarrow \infty} \frac{S_X}{\ell} = \lim_{N \rightarrow \infty} \frac{S_N}{N}, \quad (65)$$

where we denoted with S_N the entropy of the full system. For pure quantum states, one has either $K_{kk} = 0$ or $K_{kk} = 1$, which implies that $S_N = 0$ and $\alpha = 0$, as it should be. This is not the case in the presence of the environment, because the global system is not pure. A similar behavior is typically observed in out-of-equilibrium generic quadratic fermionic and bosonic systems [22–25].

Let us now derive the prefactor $c(\Theta)$ of the logarithmic growth in Eq. (62). By using (37), the term in the

brackets in (57) yields

$$\frac{c(\Theta)}{3} = \lim_{\delta, \epsilon \rightarrow 0^+} \frac{1}{\pi i} \oint_{\gamma} d\lambda e(1 + \epsilon, \lambda) \frac{d(-\beta_{\lambda}^2)}{d\lambda}, \quad (66)$$

where β_{λ} is defined in Eq. (60) and, again, γ denotes the “dogbone” contour in Fig. 2. We can perform an integration by parts to obtain

$$\frac{c(\Theta)}{3} = \lim_{\delta, \epsilon \rightarrow 0^+} \frac{1}{8\pi^3 i} \oint_{\gamma} d\lambda \ln^2 \left(\frac{\lambda + \Theta}{\lambda - \Theta} \right) \ln \left(\frac{1 + \epsilon + \lambda}{1 + \epsilon - \lambda} \right). \quad (67)$$

The contribution of the circles around ± 1 in γ (see Fig. 2) vanish in the limit $\epsilon \rightarrow 0^+$. The integration along the horizontal paths can be performed using the fact that, for $\delta \rightarrow 0^+$, one has

$$\ln \left(\frac{x \pm i\delta + t}{x \pm i\delta - t} \right) \rightarrow \ln \left| \frac{t + x}{t - x} \right| \mp i\pi \text{sgn}(t) \Theta_H(|t| - |x|). \quad (68)$$

Finally, the integral (67) gives

$$c(\Theta) = \frac{3}{2\pi^2} \int_{-\Theta}^{\Theta} dx \log \left(\frac{\Theta + x}{\Theta - x} \right) \log \left(\frac{1 + x}{1 - x} \right), \quad (69)$$

which can be performed analytically, yielding

$$\begin{aligned} c(\Theta) &= \\ &\frac{3}{\pi^2} \left\{ \text{Li}_2 \left(\frac{2\Theta}{\Theta - 1} \right) + \text{Li}_2 \left(\frac{2\Theta}{\Theta + 1} \right) + 2\Theta \text{Re} \left[\text{Li}_2 \left(\frac{1 + \Theta}{1 - \Theta} \right) \right] \right. \\ &\left. - \frac{1}{3} \pi^2 \Theta + \frac{\Theta}{2} \ln \left(\frac{(1 - \Theta)^3 (1 + \Theta)}{16\Theta^4} \right) \ln \left(\frac{1 - \Theta}{1 + \Theta} \right) \right\}. \end{aligned} \quad (70)$$

Here $\text{Li}_n(z)$ is the polylogarithm function [50]. In particular, $\text{Li}_2(x)$ is

$$\text{Li}_2(x) := - \int_0^x dz \frac{\ln(1 - z)}{z}. \quad (71)$$

In Eq. (70) we restricted ourselves to $0 \leq \Theta \leq 1$ because $c(\Theta)$ is an even function of Θ , as is clear from Eq. (69). This result is somewhat reminiscent of the effective central charge obtained in free fermion chains in the presence of defects [51–55].

In the limit $\Theta \rightarrow 1$ one recovers the case without baths. Thus, Eq. (70) gives the central charge $c = 1$ of the model. For $\Theta \rightarrow 1$, which corresponds to a low-temperature limit, one has

$$\begin{aligned} c(\Theta) &= 1 + \frac{\Theta - 1}{2\pi^2} \left\{ 6 + 2\pi^2 + 3 \ln^2(2) + 6 \ln(2) \right. \\ &\left. + 3 \left[\ln \left(\frac{1 - \Theta}{4} \right) - 2 \right] \ln(1 - \Theta) \right\} + \mathcal{O}((\Theta - 1)^2). \end{aligned} \quad (72)$$

Notice the logarithmic term $\ln(1 - \Theta)$. In the opposite limit $\Theta \rightarrow 0$ one obtains that $c(\Theta)$ vanishes as

$$c(\Theta) = \frac{1}{\pi^2} \left(6\Theta^2 + \frac{4}{3}\Theta^4 \right) + \mathcal{O}(\Theta^6). \quad (73)$$

The results derived so far hold for $|h| < 2$. Away from this region, i.e., for $|h| > 2$, the von Neumann entropy is given by (62) with $c = 0$ and α given by (64). The behavior of $c(\Theta)$ as a function of Θ is illustrated in Fig. 3.

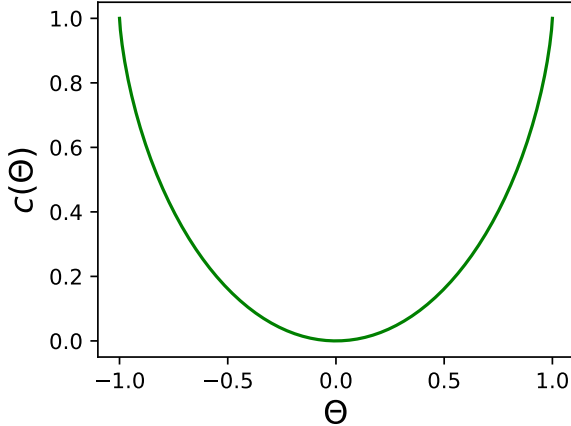


Figure 3. Effective central charge $c(\Theta)$ for the tight-binding chain coupled to localized thermal baths. Here $\Theta \in [-1, 1]$ encodes the information about the baths. For a single bath at the left edge of the chain, Θ is given by Eq. (77). For two baths at the edges of the chain, Θ is given by Eq. (81). In the limit $|\Theta| \rightarrow 1$, one recovers the CFT result $c = 1$. For $\Theta = 0$ one has $c \rightarrow 0$, which corresponds to a high-temperature limit.

2. Open boundary conditions

Let us now discuss the case with OBC and consider a block of ℓ sites starting at one edge of the chain [see Fig. 1 (a)]. Now, one has $\zeta = 1$ in the fermionic correlator (52), which has the Toeplitz-plus-Hankel structure with the same symbol. A version of the Fisher-Hartwig conjecture for Toeplitz-plus-Hankel matrices exists [38], and the analysis can be carried out as for PBC. However, the application of the Fisher-Hartwig conjecture is more cumbersome and we do not report the details. Following the approach of Ref. [39] we obtain that

$$S_X = \alpha\ell + \frac{c(\Theta)}{6} \ln(\ell) + \mathcal{O}(1), \quad (74)$$

where $c(\Theta)$ is the same as in Eq. (62).

A. Single bath

To illustrate our results, we first focus on the open tight-binding chain with only one edge coupled to the environment (see Fig. 1) and $|h| < 2$. In the steady state, from Eq. (51) we have

$$K_{kq} = \langle b_k^\dagger b_q \rangle = \delta_{kq} f(\omega_k), \quad (75)$$

where b_k are the Bogoliubov operators of Eq. (5), ω_k their single-particle energies [cf. Eq. (10)], and $f(\omega_k)$ the Fermi-Dirac distribution describing the bath [cf. Eq. (44)]. Eq. (75) implies that the function θ_{kk} [cf. (28)] is given by

$$\theta_{kk} = 1 - 2f(\omega_k). \quad (76)$$

The prefactor of the logarithmic contribution in the von Neumann entropy [cf. (62)] depends on the value of θ_{kk} at the Fermi point k_F [cf. (60)]. Thus, we have

$$\Theta := \theta_{kk}|_{k=k_F} = 1 - 2f(0) = \tanh\left(-\frac{\mu_L}{2T_L}\right). \quad (77)$$

Notice that Θ depends only on the ratio μ_L/T_L . The limit $\mu_L/T_L \rightarrow 0$ gives $\Theta \rightarrow 0$ and a vanishing $c(\Theta)$ (see Fig. 3). In the limit $\mu_L/T_L \rightarrow 0$ the logarithmic correction to the entropy disappears. Specifically, from (73) we find that $c(\Theta) \sim (\mu_L/T_L)^2$. This regime corresponds to either infinite temperature $T_L \rightarrow \infty$ or vanishing chemical potential $\mu_L \rightarrow 0$. On the other hand, for $|\mu_L/T_L| \rightarrow \infty$ we have $|\Theta| \rightarrow 1$ and $c \rightarrow 1$. Moreover, in this limit $K_{kk} \rightarrow 0$ or $K_{kk} \rightarrow 1$, which implies that $\alpha \rightarrow 0$ [cf. (64)]. Thus, [see Eq. (74)] we recover the ground-state scaling of the von Neumann entropy.

B. Two baths

Let us now discuss the case with two different thermal baths, first considering the simpler case of PBC with the baths placed at sites $n = 1$ and $n = N/2$ [see Fig. 1 (b)]. Under the assumption that the spectral density $J(\omega)$ [cf. (46)] is the same for the two baths, we have for the couplings

$$\gamma_{L,k} = \gamma_{R,k} = \frac{J(\omega_k)}{N}, \quad (78)$$

since, from Eq. (12a), we have $|\phi_{1k}|^2 = |\phi_{Nk}|^2 = 1/N$. Using Eq. (51), we thus obtain

$$K_{kq} = \delta_{kq} \frac{f_L(\omega_k) + f_R(\omega_k)}{2}, \quad (79)$$

$$\theta_{kk} = \frac{1}{2} \left[\tanh\left(\frac{\omega_k - \mu_L}{2T_L}\right) + \tanh\left(\frac{\omega_k - \mu_R}{2T_R}\right) \right]. \quad (80)$$

Notice that the correlator K_{kq} does not depend on the couplings $\gamma_{L/R,k}$. Moreover, as is clear from (79), the steady-state correlator is written in terms of the average between the Fermi-Dirac distributions describing the baths. From Eq. (80) we obtain

$$\Theta = \frac{1}{2} \left[\tanh\left(-\frac{\mu_L}{2T_L}\right) + \tanh\left(-\frac{\mu_R}{2T_R}\right) \right]. \quad (81)$$

Notice that Θ depends only the ratios μ_L/T_L and μ_R/T_R , which is structurally similar to what we obtained in the single-bath scenario.

In the case of OBC and baths placed at the edges of the chain [see Fig. 1 (a)], one has for the couplings

$$\gamma_{L,k} = J(\omega_k) \frac{2 \sin^2(k)}{N+1}, \quad (82a)$$

$$\gamma_{R,k} = J(\omega_k) \frac{2 \sin^2(kN)}{N+1}. \quad (82b)$$

Making use of the quantization condition on k , one can show with a straightforward calculation that Eqs. (79), (80), and (81) continue to remain valid.

V. SCALING OF ENTROPY IN THE KITAEV CHAIN

We now turn to the steady-state von Neumann entropy in the Kitaev chain with PBC. The blocks of the Majorana correlation matrix Γ [cf. Eq. (32)] read as

$$\Pi_{nm} = \int_{-\pi}^{\pi} \frac{dk}{2\pi} \begin{bmatrix} 0 & \theta_{kk} e^{-i\xi(k)} \\ -\theta_{kk} e^{i\xi(k)} & 0 \end{bmatrix} e^{ik(n-m)}, \quad (83)$$

where $\xi(k)$ is defined in Eq. (21) and θ_{kk} is the same as in Eq. (80). Notice that for $\mu_L = \mu_R = 0$ and $T_L = T_R = T$ one recovers the correlator for the finite-temperature Kitaev (and Ising) chain [56–58] at temperature T . For $T \rightarrow 0$ one has that $\theta_{kk} \rightarrow 1$, thus recovering the zero-temperature correlator of the Kitaev chain. Importantly, the presence of μ_L and μ_R in (80) implies that the statistical ensemble describing the steady state is not the usual finite-temperature ensemble of the Kitaev chain. For the following it is important to stress that the function $\xi(k)$ has jump discontinuities for $|h| = 2$, which determine the ground-state critical properties of the system.

Now, Eq. (83) defines a Toeplitz matrix. Given a subsystem A , we are interested in the matrix $\lambda \mathbb{1} - i\Gamma_A$ [cf. Eq. (36)], which is then also of the Toeplitz type. Let us define its symbol $g_\lambda(k)$ (cf. (83)) as

$$g_\lambda(k) := \begin{bmatrix} \lambda & -i\theta_{kk} e^{-i\xi(k)} \\ i\theta_{kk} e^{i\xi(k)} & \lambda \end{bmatrix}. \quad (84)$$

In contrast with the tight-binding chain, for which it was a scalar, now the symbol is a two-by-two matrix. At zero temperature, the asymptotic behavior in the large- ℓ limit of the Toeplitz matrix (83) has been obtained in Ref. [40]. Here we are only interested in the logarithmic correction to the volume-law scaling of the von Neumann entropy. Thus, we can use the techniques of Refs. [59, 60]. The idea is that since the logarithmic correction depends only on the singularities of the symbol, we are allowed to modify the latter, provided that we do not change its singularity structure. This eventually allows one to work with a scalar symbol.

To proceed, let us define the modified symbol $\tilde{g}_\lambda(k)$ as

$$\tilde{g}_\lambda(k) := \begin{bmatrix} \lambda & -i\theta_{kk} e^{-i|\xi(k)|} \\ i\theta_{kk} e^{i|\xi(k)|} & \lambda \end{bmatrix}, \quad (85)$$

which differs from $g_\lambda(k)$ in (84) because of the absolute value $|\xi(k)|$ in the phase factors. Its inverse $\tilde{g}_\lambda^{-1}(k)$ is

$$\tilde{g}_\lambda^{-1}(k) = \frac{1}{\lambda^2 - \theta_{kk}^2} \begin{bmatrix} \lambda & i\theta_{kk} e^{-i|\xi(k)|} \\ -i\theta_{kk} e^{i|\xi(k)|} & \lambda \end{bmatrix}. \quad (86)$$

Crucially, both \tilde{g}_λ and its inverse are smooth functions of k . As a consequence, in the limit $\ell \rightarrow \infty$, the corresponding Toeplitz determinants $D_\ell[\tilde{g}_\lambda]$ and $D_\ell[\tilde{g}_\lambda^{-1}]$ do not contain logarithmic terms. Their asymptotic behavior is determined by the Szegő-Widom theorem [61]. Given a

generic smooth symbol $z(k)$ of a Toeplitz matrix, the Szegő-Widom theorem gives

$$\ln D_\ell[z] = \ell \int_{-\pi}^{\pi} \frac{dk}{2\pi} \ln \det(z(k)) + \mathcal{O}(1). \quad (87)$$

In our case we have $z(k) = \tilde{g}_\lambda(k)$ or $\tilde{g}_\lambda^{-1}(k)$. Moreover, we can use the so-called Basor localization theorem [62], which allows to write, in the limit $\ell \rightarrow \infty$,

$$\ln D_\ell[g_\lambda] = \ln D_\ell[g_\lambda \tilde{g}_\lambda^{-1}] - \ln D_\ell[\tilde{g}_\lambda^{-1}] + \mathcal{O}(1). \quad (88)$$

Here the first contribution contains logarithmic terms, whereas the second one gives rise to volume-law terms as in (87). To proceed, let us now notice that

$$g_\lambda \tilde{g}_\lambda^{-1} = \frac{1}{\lambda^2 - \theta_{kk}^2} \begin{bmatrix} \lambda^2 - \theta_{kk}^2 e^{i(|\xi| - |\xi|)} & i\lambda \theta_{kk} (e^{-i|\xi|} - e^{-i|\xi|}) \\ i\lambda \theta_{kk} (e^{i|\xi|} - e^{i|\xi|}) & \lambda^2 - \theta_{kk}^2 e^{i(|\xi| - |\xi|)} \end{bmatrix}. \quad (89)$$

If $-\pi \leq k \leq 0$, then $\xi(k) \geq 0$ and $g_\lambda \tilde{g}_\lambda^{-1}$ is the identity matrix. On the other hand, if $0 < k \leq \pi$, then $\xi(k) < 0$ and Eq. (89) becomes

$$g_\lambda \tilde{g}_\lambda^{-1} = \frac{1}{\lambda^2 - \theta_{kk}^2} \begin{bmatrix} \lambda^2 - \theta_{kk}^2 e^{-2i\xi} & -2\lambda \theta_{kk} \sin(\xi) \\ -2\lambda \theta_{kk} \sin(\xi) & \lambda^2 - \theta_{kk}^2 e^{2i\xi} \end{bmatrix}. \quad (90)$$

Diagonalizing the matrix in (90), one obtains that the eigenvalues b_\pm are

$$b_\pm = \left[\frac{\sqrt{\lambda^2 - \theta_{kk}^2} \cos^2(\xi) \pm |\theta_{kk} \sin(\xi)|}{\sqrt{\lambda^2 - \theta_{kk}^2}} \right]^2. \quad (91)$$

One can easily verify that the corresponding eigenvectors are smooth functions of k . Hence, a further application of Basor localization theorem yields

$$\ln D_\ell[g_\lambda \tilde{g}_\lambda^{-1}] = \ln D_\ell[b_-] + \ln D_\ell[b_+] + \mathcal{O}(1). \quad (92)$$

Here we also used that, according to the Szegő-Widom theorem (87), the contribution in Eq. (92) of the matrices that diagonalize (90) would be a constant that we can neglect in the limit $\ell \rightarrow \infty$, because it is subleading. Now in (92), $D_\ell[b_\pm]$ are determinants of Toeplitz matrices with scalar symbols. Their asymptotic behavior for large ℓ can be determined by using the Fisher-Hartwig conjecture for scalar symbols (as in section IV). We obtain

$$\begin{aligned} \ln D_\ell[b_\pm] &= \ell \int_{-\pi}^{\pi} \frac{dk}{2\pi} \ln b_\pm(k) \\ &\quad + \ln^2 \left[\frac{\sqrt{\lambda^2 \pm |\Theta|}}{\sqrt{\lambda^2 - \Theta^2}} \right] \frac{\ln(\ell)}{\pi^2} + \mathcal{O}(1), \end{aligned} \quad (93)$$

where

$$\Theta = \begin{cases} \theta_{kk}|_{k=\pi} & \text{for } h = 2, \\ \theta_{kk}|_{k=0} & \text{for } h = -2. \end{cases} \quad (94)$$

Since ϕ_{nk} for the Kitaev chain has the same form of the corresponding quantity for the tight-binding chain, one

can see that in both cases Θ is given by Eq. (77) for the geometry with only one edge of the chain coupled to the environment and by Eq. (81) with two baths. Noticing that $b_- b_+ = 1$, and using Eqs. (87), (88), (93), we get

$$\begin{aligned} \ln D_\ell[g_\lambda] &= \ell \int_{-\pi}^{\pi} \frac{dk}{2\pi} \ln(\lambda^2 - \theta_{kk}^2) \\ &+ \ln^2 \left[\frac{\sqrt{\lambda^2 + |\Theta|}}{\sqrt{\lambda^2 - \Theta^2}} \right] \frac{2 \ln(\ell)}{\pi^2} + \mathcal{O}(1). \end{aligned} \quad (95)$$

We can now determine the scaling of the steady-state von Neumann entropy. The von Neumann entropy of a subsystem A of size ℓ embedded in an infinite periodic chain in the large ℓ limit is given by

$$S_A = \alpha \ell + \frac{c(\Theta)}{3} \ln(\ell) + \mathcal{O}(1). \quad (96)$$

Equation (96) has the same form of Eq. (62), although α and $c(\Theta)$ are not the same. The coefficient α of the volume-law term is easily obtained by using (37):

$$\alpha = \int_{-\pi}^{\pi} \frac{dk}{2\pi} e(1, \theta_{kk}), \quad (97)$$

where $e(x, \lambda)$ is defined in Eq. (35). Eq. (97) is obtained after replacing the first term of (95) in (37). Equation (97) has the same structure as for the tight-binding chain [cf. Eq. (64)]. Specifically, α is the density of von Neumann entropy of the full system.

Let us now discuss the prefactor $c(\Theta)$ of the logarithmic term in Eq. (96). By substituting the second term of (95) in (37), we obtain

$$\frac{c(\Theta)}{3} = \lim_{\delta, \epsilon \rightarrow 0^+} \oint_\gamma \frac{d\lambda}{4\pi^3 i} \ln\left(\frac{1 + \epsilon + \lambda}{1 + \epsilon - \lambda}\right) \ln^2\left(\frac{\sqrt{\lambda^2 + |\Theta|}}{\sqrt{\lambda^2 - \Theta^2}}\right). \quad (98)$$

As for the tight-binding chain, γ is the same dogbone contour of Fig. 2. After using (68), and proceeding as for the tight-binding chain (cf. section IV), we obtain

$$c(\Theta) = \frac{3}{4\pi^2} \int_{-\Theta}^{\Theta} dx \ln\left(\frac{1+x}{1-x}\right) \ln\left(\frac{\Theta+x}{\Theta-x}\right). \quad (99)$$

Remarkably, Eq. (99) is half of the result of Eq. (69) obtained for the tight-binding chain. Clearly, in the zero-temperature limit one recovers the well-known central charge $c = 1/2$ of the critical Kitaev chain.

VI. NUMERICAL RESULTS

We now provide numerical benchmarks for the results of Sec. IV and Sec. V. In Sec. VI A we overview the behavior of the subsystem von Neumann entropy. Our main results are contained in Sec. VI B, where we discuss the scaling behavior of steady-state mutual information both for the tight-binding chain (Sec. VI B 1) and for the Kitaev chain (Sec. VI B 2). Our numerical results confirm

a logarithmic scaling for the mutual information, being in perfect agreement with the predictions of the previous sections. We should stress again that even though the mutual information is not a proper measure of entanglement, we numerically checked that the logarithmic scaling also occurs with the fermionic entanglement negativity [26], thus suggesting that the growth of the mutual information reflects logarithmic entanglement growth.

A. Volume-law scaling of von Neumann entropy

In the presence of the external baths, the steady-state von Neumann entropy exhibits a volume-law scaling as $\alpha\ell$, with ℓ being the size of the subsystem. The prefactor α is given by Eq. (64) for the tight-binding chain and by Eq. (97) for the Kitaev chain. For both models, α is the density of the von Neumann entropy of the full system. In the absence of baths, the full system is in a pure state, and its von Neumann entropy is zero ($\alpha = 0$). The volume-law scaling is due to the fact that the steady state is described by a finite-temperature-like statistical ensemble. Here we focus on the tight-binding chain with OBC and one thermal bath (see Fig. 1 (a)). Results for different boundary conditions and for the Kitaev chain are qualitatively similar and will not be discussed.

Figure 4 reports the von Neumann entropy S_A as a function of the chain length N , where the subsystem A is the half-chain with $\ell = N/2$ [Fig. 1(a)]. Only the left edge is in contact with a thermal bath at $\mu_L = -1$ and temperature T_L . Data in the figure correspond to different temperatures $T_L = T$. A robust growth is visible at all temperatures, with a slope that decreases as the temperature is lowered. This is expected, since at $T = 0$ the scaling of the von Neumann entropy is logarithmic with

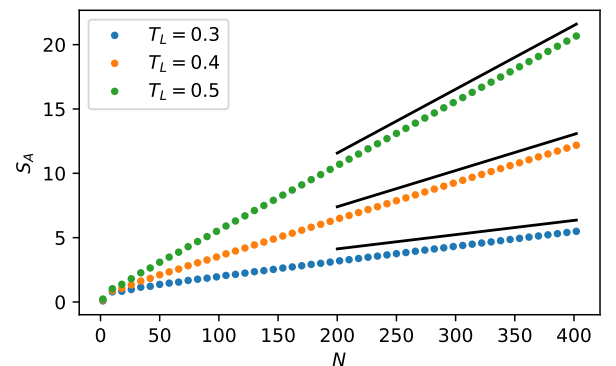


Figure 4. Volume-law scaling of the von Neumann entropy in the open tight-binding chain with a single bath on the left edge of the system (see Fig. 1). Subsystem A is the half chain ($\ell = N/2$). Here we choose $h = 1$, $\mu_L = -1$, and $T_L = 0.3, 0.4, 0.5$. Straight lines denote the analytic predictions for the volume-law scaling, in the limit $\ell \rightarrow \infty$ [cf. Eq. (62)]. The logarithmic correction is not clearly visible at this scale.

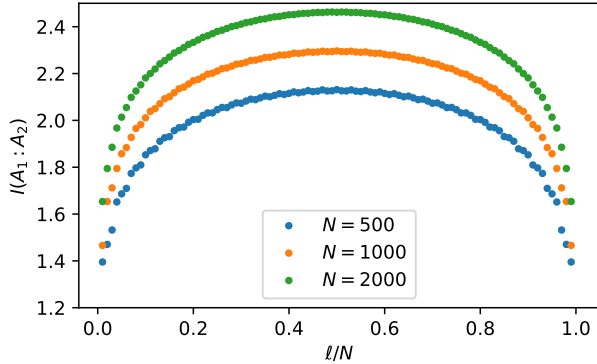


Figure 5. Mutual information $I(A_1 : A_2)$ between two intervals in the open tight-binding chain with a thermal bath on the left edge. Here we choose $\mu_L = -1$, $T_L = 0.3$, and $h = 1$. Different colors correspond to different chain length N . The data are plotted versus ℓ/N , with ℓ being the size of A_1 (see Fig. 1 (a)). Notice the symmetry under exchange of the two subsystems $\ell \leftrightarrow N - \ell$.

the interval size. Continuous lines show the expected linear behavior as $\alpha\ell$ in the limit $\ell \rightarrow \infty$, with a prefactor α given by Eq. (64). We observe a qualitative agreement with the theoretical predictions, at least to the leading order in ℓ . However, as also expected from Eq. (62), subleading logarithmic corrections are present. To reveal them it is convenient to use the mutual information.

B. Logarithmic scaling of mutual information

We now discuss the scaling of the steady-state mutual information in the presence of external baths. The logarithmic prefactor is determined by the singular structure of the single-particle energy dispersion, as discussed in Sec. IV and Sec. V.

1. Tight-binding chain

For the tight-binding model of Eq. (9), we consider the same setup as in Sec. IV A, i.e. the open chain with a thermal bath on the left edge. We fix $h = 1$, $\mu_L = -1$, and $T_L = 0.3$. Our numerical data for the mutual information $I(A_1 : A_2)$ between two complementary intervals A_1 and $A_2 = \bar{A}_1$ are plotted in Fig. 5 versus ℓ/N , with ℓ being the size of A_1 . The three different data sets correspond to different values of N . At each fixed N , $I(A_1 : A_2)$ increases upon increasing ℓ up to $\ell \sim N/2$, after which it starts decreasing. The behavior at intermediate $1 \ll \ell \ll N$ is consistent with a logarithmic increase, as predicted in Eq. (74), which should hold in the limit $N \rightarrow \infty$ and then $\ell \rightarrow \infty$ (with this order of limits).

Looking now at the definition of the mutual information [cf. Eq. (1)], it is clear that, when constructing $I(A_1 : A_2)$, the volume-law terms in the entropies cancel out. To derive the prefactor of the logarithmic scaling, we can use Eq. (74) for each term appearing in (1). Notice that no logarithmic contribution is expected from $S_{A_1 \cup A_2}$, since the entropy of the full system for large N is exactly αN , with α given by (64). Let us also stress that, in principle, we are not allowed to use Eq. (74) for S_{A_2} because the size $N - \ell$ of A_2 is comparable with N . To proceed, we should then conjecture a generalization for an interval A of generic size, embedded in a finite-size chain. Following the standard strategy for critical systems described by CFTs, we write [63]

$$S_A = \alpha\ell + \frac{c(\Theta)}{6} \ln \left[\frac{N}{\pi} \sin \left(\frac{\pi\ell}{N} \right) \right] + \mathcal{O}(1). \quad (100)$$

Notice that the prefactor of the volume-law term is the same as before, while in the logarithmic term of Eq. (74) we replaced

$$\ell \rightarrow X_\ell, \quad \text{with } X_\ell := \frac{N}{\pi} \sin \left(\frac{\pi\ell}{N} \right), \quad (101)$$

where X_ℓ is the so-called chord length. Eq. (100) holds in the thermodynamic limit $\ell, N \rightarrow \infty$. For systems with boundaries, as is the case here, the chord length differs from (101) by an overall factor 2, which only affects the $\mathcal{O}(1)$ term, and can therefore be neglected. We conclude that

$$I(A_1 : A_2) = \frac{c(\Theta)}{3} \ln \left[\frac{N}{\pi} \sin \left(\frac{\pi\ell}{N} \right) \right] + \mathcal{O}(1). \quad (102)$$

The factor 1/3 rather than 1/6 is due to the fact that both subsystems A_1 and A_2 contribute with a logarithmic term. Importantly, Eq. (102) implies that for large ℓ, N the data for the mutual information should collapse on the same curve, when plotted as a function of X_ℓ .

The validity of Eq. (102) is investigated in Fig. 6 for the tight-binding chain with one thermal bath on the left edge. We consider two different temperatures $T_L = 0.3, 0.5$ at fixed $\mu_L = -1$. The mutual information $I(A_1 : A_2)$ is plotted versus X_ℓ (notice the logarithmic scale on the x -axis) for several values of $N = 200, 600, 1000$. For both temperatures, the data exhibit collapse. The quality of the collapse improves upon increasing N , as expected. Continuous lines are fits to Eq. (102), where $c(\Theta)$ is kept fixed and given by Eq. (70), while the additive $\mathcal{O}(1)$ term being the only fitting parameter. For both temperatures, the agreement between the data and the fits is very satisfactory.

Eq. (102) also implies that, for large N , the mutual information between the two halves of the chain scales logarithmically as $c(\Theta) \ln(N)/3$. This is shown in Fig. 7, for the same setup as in Fig. 6. The various data sets correspond to different temperatures of the external bath. The logarithmic increase is clearly visible (notice the semilog

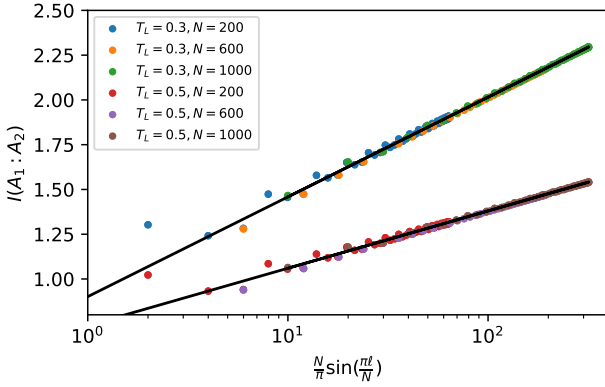


Figure 6. Mutual information $I(A_1 : A_2)$ between two complementary intervals [see Fig. 1 (a)] in the open tight-binding chain with a thermal bath on the left edge. On the x -axis $N \sin(\pi\ell/N)/\pi \equiv X_\ell$ is the chord length. Data are for fixed $\mu_L = 1$, $h = 1$, and for $T_L = 0.3, 0.5$, while the various colors denote different N . The lines are fits to $c(\Theta) \ln(X_\ell)/3 + b$, $c(\Theta)$ being the effective central charge [cf. Eq. (70)] and b a fitting constant parameter.

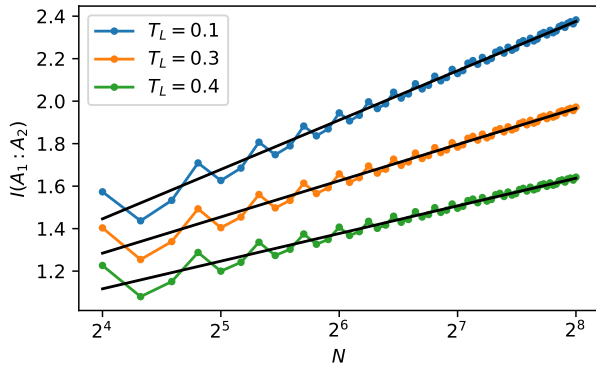


Figure 7. Scaling of the half-chain mutual information in the open tight-binding chain with a thermal bath of the left edge of the chain. Here we fix $\mu_L = -1$, $h = 1$. Different colors are for different values of T_L . Continuous lines are fits to $a \ln(N) + b$, with a, b fitting parameters.

scale), although oscillating corrections are present. The continuous lines are fits to

$$I(A_1 : A_2) = a \ln(N) + b, \quad (103)$$

with a, b fitting parameters. Further checks of our results are provided in Fig. 8 where, for each temperature, we numerically extract $c(\Theta)$ by fitting the mutual information to Eq. (103). Symbols are the results of the fits, which are obtained as in Fig. 7 fitting the data with $N > 2^6$. At low temperature, one finds $c(\Theta) \rightarrow 1$, whereas $c(\Theta)$ vanishes in the high-temperature limit. The continuous line is the analytic prediction in the limit $N \rightarrow \infty$, given by Eq. (70). The agreement with the numerics is excellent.

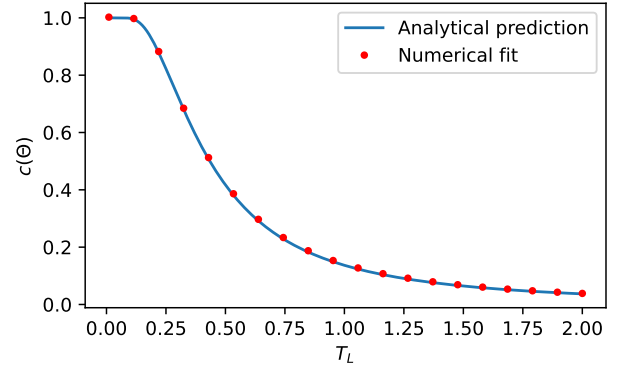


Figure 8. The effective central charge $c(\Theta)$ versus the temperature T_L , as obtained from fits of numerical data as those in Fig. 7. Parameters are the same as in Fig. 7.

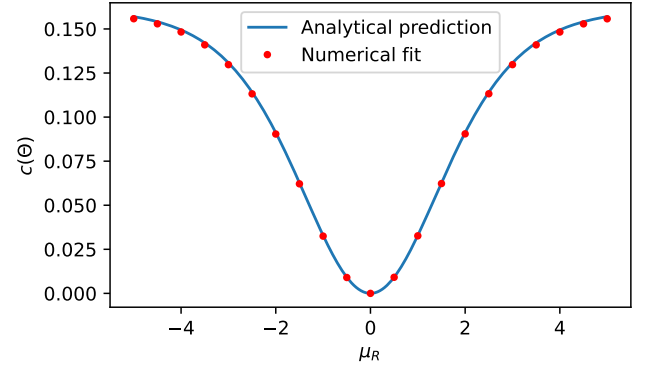


Figure 9. Logarithmic scaling of the mutual information $I(A_1 : A_2)$ in the tight-binding chain with OBC coupled to two thermal baths at the edges. We plot the effective central charge $c(\Theta)$ of the logarithmic growth versus the chemical potential μ_R of the right bath. Here we fix $h = 1$, $\mu_L = 0$, and $T_L = T_R = 1$. Numerical results for $c(\Theta)$ are obtained by performing a finite-size scaling analysis for the half-chain mutual information.

Finally we discuss a two-bath geometry, where the edges of the chain are connected to two different thermal baths. Here we fix $h = 1$, $\mu_L = 0$, $T_L = T_R = 1$, and vary μ_R . In Fig. 9 we plot the numerically extracted $c(\Theta)$ versus μ_R . As for Fig. 8, the continuous line denotes the theoretical result in the limit $N \rightarrow \infty$, which is in perfect agreement with the numerics.

2. Kitaev chain

We conclude by discussing the steady-state mutual information in the Kitaev chain. Here we consider a PBC geometry, as depicted in Fig. 1 (b). Two sites at mutual distance $N/2$ are put in contact with two external baths at temperatures $T_{R/L}$ and with chemical potential $\mu_{R/L}$.

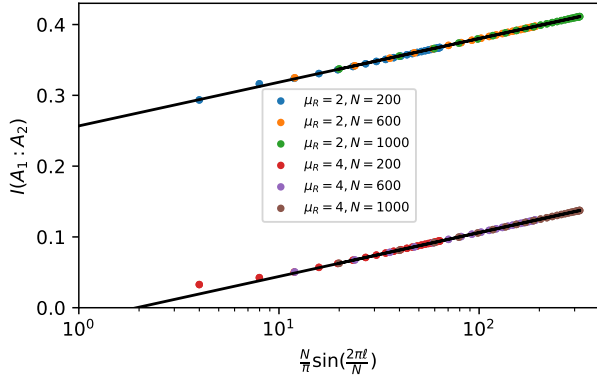


Figure 10. Mutual information $I(A_1 : A_2)$ between two intervals in the Kitaev chain with PBC and two external baths (see Fig. 1) versus the chord length $X_{2\ell} = N \sin(2\pi\ell/N)/\pi$. Here we choose $T_L = T_R = 1$, $\mu_L = 0$ and $\mu_R = 2, 4$. The various symbols correspond to different chain sizes N . Continuous lines are fits to $I(A_1 : A_2) = c(\Theta) \ln(X_{2\ell})/6 + b$, with $c(\Theta)$ the effective central charge, and b a fitting constant.

We choose $T_L = T_R = 1$, $\mu_L = 0$, $\mu_R = 2, 4$, and fix $h = 2$. We consider the mutual information $I(A_1 : A_2)$ between two intervals of size ℓ and $N/2 - \ell$ placed between the baths (see Fig. 1). First, we should observe that in constructing the mutual information (1) all the entropies (i.e., S_{A_1} , S_{A_2} , and $S_{A_1 \cup A_2}$) contain a subleading logarithmic term. This happens because $S_{A_1 \cup A_2}$ is not the full system. As for the tight-binding chain the volume-law terms cancel out. The final result is

$$I(A_1 : A_2) = \frac{c'(\Theta)}{3} \ln(X_{2\ell}) + \mathcal{O}(1), \quad (104)$$

where $X_{2\ell}$ is the chord length in Eq. (101) (notice the factor 2), and

$$c'(\Theta) = \frac{c(\Theta)}{2}. \quad (105)$$

Here $c(\Theta)$ is given in Eq. (70) and Θ depends on the parameters of baths (cf. Eq. (81)). The factor 1/2 in Eq. (105) reflects the fact that the prefactor of the logarithmic growth for the Kitaev chain is half that of the tight-binding chain, as derived in Sec. V. To derive Eq. (104) we used the fact that, for all the intervals A_1 , A_2 , and $A_1 \cup A_2$,

$$S_W \xrightarrow{\ell, N \rightarrow \infty} \frac{c'(\Theta)}{3} \ln(X_\ell), \quad W = A_{1(2)}, A_1 \cup A_2, \quad (106)$$

where X_ℓ is the chord length and $c'(\Theta)$ is given by Eq. (105). After substituting (106) in the definition of the mutual information (1), we obtain (104). We point out that Eq. (104) holds only for the geometry in Fig. 1

(b), although it could be easily generalized to more general settings.

The validity of Eq. (104) is numerically verified in Fig. 10, where we plot $I(A_1 : A_2)$ versus $X_{2\ell}$. For both values of μ_R , the data exhibit collapse at large ℓ, N . Continuous lines are fits to Eq. (104), the only fitting parameter being the $\mathcal{O}(1)$ constant, whereas $c'(\Theta)$ is given by Eq. (105). The agreement between the analytic prediction in the scaling limit $\ell, N \rightarrow \infty$ and the numerics is nearly perfect already for relatively small chains with $X_{2\ell} \sim 10$.

VII. CONCLUSIONS

We investigated the quantum-information spreading in the tight-binding chain and the Kitaev chain in the presence of external thermal baths coupled to individual sites of the chains. To this purpose, we employed a self-consistent *nonlocal* Lindblad master equation approach, where the Lindblad operators modeling the baths are written in terms of the Bogoliubov modes that diagonalize the isolated system, implying that they are, in principle, nonlocal in real space [16]. The statistical ensemble describing the steady state is written in terms of a convex combination of the Fermi-Dirac distributions of the baths. We showed that the steady-state von Neumann entropy of a subsystem exhibits a volume-law scaling with the subsystem size, reflecting that the system is not in a pure state. The mutual information exhibits an area-law scaling for generic values of the system parameters. Interestingly, we observe logarithmic violations of the area law in the presence of ground-state criticality. This behavior reflects the singularity of the single-particle energy dispersion of the models, which is present at all energies. We analytically derived the prefactor of the logarithmic growth of the mutual information, which depends on the system and bath parameters, such as the temperature and the chemical potential.

Let us now mention some promising directions for future work. First of all, here we only analyzed the steady-state value of the mutual information: it would be tempting to study the full-time dynamics, in order to establish how the logarithmic scaling builds up during the evolution of the system. A natural conjecture is that the same effective central charge governs a logarithmic increase in time, as in Ref. [31]. Our analysis may be also extended to genuine quantum entanglement measures for mixed states, such as the fermionic logarithmic negativity. Finally, it would be important to check the validity of our results by comparing them with *ab initio* numerical simulations, or with results obtained using different master equations. A crucial question to address is whether the logarithmic scaling of the mutual information would survive in interacting integrable systems or even in non-integrable ones.

[1] W. H. Zurek, Decoherence, einselection, and the quantum origins of the classical, *Review of Modern Physics* **75**, 715 (2003).

[2] D. Rossini and E. Vicari, Coherent and dissipative dynamics at quantum phase transitions, *Physics Reports* **936**, 1 (2021).

[3] N. Syassen, D. M. Bauer, M. Lettner, T. Volz, D. Dietze, J. J. García-Ripoll, J. I. Cirac, G. Rempe, and S. Dürr, Strong dissipation inhibits losses and induces correlations in cold molecular gases, *Science* **320**, 1329 (2008).

[4] Y. Lin, J. P. Gaebler, F. Reiter, T. R. Tan, R. Bowler, A. S. Sørensen, D. Leibfried, and D. J. Wineland, Dissipative production of a maximally entangled steady state of two quantum bits, *Nature* **504**, 415 (2013).

[5] S. Diehl, A. Micheli, A. Kantian, B. Kraus, H. P. Büchler, and P. Zoller, Quantum states and phases in driven open quantum systems with cold atoms, *Nature Physics* **4**, 878 (2008).

[6] F. Verstraete, M. M. Wolf, and J. Ignacio Cirac, Quantum computation and quantum-state engineering driven by dissipation, *Nature Physics* **5**, 633 (2009).

[7] J. Eisert and T. Prosen, Noise-driven quantum criticality (2010), arXiv:1012.5013 [quant-ph].

[8] M. Roncaglia, M. Rizzi, and J. I. Cirac, Pfaffian state generation by strong three-body dissipation, *Physical Review Letters* **104**, 096803 (2010).

[9] S. Diehl, E. Rico, M. A. Baranov, and P. Zoller, Topology by dissipation in atomic quantum wires, *Nature Physics* **7**, 971 (2011).

[10] I. Bouchoule, B. Doyon, and J. Dubail, The effect of atom losses on the distribution of rapidities in the one-dimensional bose gas, *SciPost Physics* **9**, 044 (2020).

[11] D. Rossini, A. Ghermaoui, M. B. Aguilera, R. Vatré, R. Bouanne, J. Beugnon, F. Gerbier, and L. Mazza, Strong correlations in lossy one-dimensional quantum gases: From the quantum zeno effect to the generalized gibbs ensemble, *Physical Review A* **103**, L060201 (2021).

[12] K. Seetharam, A. Leroose, R. Fazio, and J. Marino, Correlation engineering via nonlocal dissipation, *Phys. Rev. Research* **4**, 013089 (2022).

[13] G. Lindblad, On the generators of quantum dynamical semigroups, *Communications in Mathematical Physics* **48**, 119 (1976).

[14] V. Gorini, A. Kossakowski, and E. C. G. Sudarshan, Completely positive dynamical semigroups of n-level systems, *Journal of Mathematical Physics* **17**, 821 (1976), <https://aip.scitation.org/doi/pdf/10.1063/1.522979>.

[15] H. P. Breuer and F. Petruccione, *The theory of open quantum systems* (Oxford University Press, Great Clarendon Street, 2002).

[16] A. D'Abbruzzo and D. Rossini, Self-consistent microscopic derivation of Markovian master equations for open quadratic quantum systems, *Phys. Rev. A* **103**, 052209 (2021).

[17] A. D'Abbruzzo and D. Rossini, Topological signatures in a weakly dissipative Kitaev chain of finite length, *Phys. Rev. B* **104**, 115139 (2021).

[18] L. Amico, R. Fazio, A. Osterloh, and V. Vedral, Entanglement in many-body systems, *Rev. Mod. Phys.* **80**, 517 (2008).

[19] P. Calabrese, J. Cardy, and B. Doyon, Entanglement entropy in extended quantum systems, *Journal of Physics A: Mathematical and Theoretical* **42**, 500301 (2009).

[20] J. Eisert, M. Cramer, and M. B. Plenio, Colloquium: Area laws for the entanglement entropy, *Rev. Mod. Phys.* **82**, 277 (2010).

[21] N. Laflorencie, Quantum entanglement in condensed matter systems, *Physics Reports* **646**, 1 (2016).

[22] V. Alba and F. Carollo, Spreading of correlations in Markovian open quantum systems, *Phys. Rev. B* **103**, L020302 (2021).

[23] F. Carollo and V. Alba, Dissipative quasiparticle picture for quadratic Markovian open quantum systems, *Phys. Rev. B* **105**, 144305 (2022).

[24] V. Alba and F. Carollo, Hydrodynamics of quantum entropies in Ising chains with linear dissipation, *Journal of Physics A: Mathematical and Theoretical* **55**, 74002 (2022).

[25] V. Alba and F. Carollo, Logarithmic negativity in out-of-equilibrium open free-fermion chains: An exactly solvable case (2022).

[26] G. Vidal and R. F. Werner, Computable measure of entanglement, *Physical Review A* **65**, 032314 (2002).

[27] V. Alba and F. Carollo, Noninteracting fermionic systems with localized losses: Exact results in the hydrodynamic limit, *Phys. Rev. B* **105**, 054303 (2022).

[28] V. Alba, Unbounded entanglement production via a dissipative impurity, *SciPost Phys.* **12**, 11 (2022).

[29] P. Di Francesco, P. Mathieu, and D. Senechal, *Conformal Field Theory*, Graduate Texts in Contemporary Physics (Springer-Verlag, New York, 1997).

[30] V. Eisler and Z. Zimborás, Area-law violation for the mutual information in a nonequilibrium steady state, *Physical Review A* **89**, 10.1103/physreva.89.032321 (2014).

[31] M. Kormos and Z. Zimborás, Temperature driven quenches in the Ising model: appearance of negative Rényi mutual information, *Journal of Physics A: Mathematical and Theoretical* **50**, 264005 (2017).

[32] X. Turkeshi and M. Schiró, Entanglement and correlation spreading in non-hermitian spin chains (2022).

[33] X. Turkeshi, L. Piroli, and M. Schiró, Enhanced entanglement negativity in boundary-driven monitored fermionic chains, *Phys. Rev. B* **106**, 024304 (2022).

[34] M. E. Fisher and R. E. Hartwig, Toeplitz Determinants: Some Applications, Theorems, and Conjectures, in *Advances in Chemical Physics* (John Wiley & Sons, Ltd, 1969) pp. 333–353.

[35] E. L. Basor and C. A. Tracy, The Fisher-Hartwig conjecture and generalizations, *Physica A: Statistical Mechanics and its Applications* **177**, 167 (1991).

[36] E. L. Basor and K. E. Morrison, The Fisher-Hartwig conjecture and Toeplitz eigenvalues, *Linear Algebra and Its Applications* **202**, 129 (1994).

[37] P. J. Forrester and N. E. Frankel, Applications and generalizations of Fisher–Hartwig asymptotics, *Journal of Mathematical Physics* **45**, 2003 (2004).

[38] P. Deifts, A. Its, and I. Krasovsky, Asymptotics of Toeplitz, Hankel, and Toeplitz+Hankel determinants with Fisher-Hartwig singularities, *Annals of Mathematics* **174**, 1243 (2011).

[39] M. Fagotti and P. Calabrese, Universal parity effects in the entanglement entropy of XX chains with open

boundary conditions, *Journal of Statistical Mechanics: Theory and Experiment* **2011**, P01017 (2011).

[40] B.-Q. Jin and V. E. Korepin, Quantum Spin Chain, Toeplitz Determinants and the Fisher—Hartwig Conjecture, *Journal of Statistical Physics* **116**, 79 (2004).

[41] E. Lieb, T. Schultz, and D. Mattis, Two soluble models of an antiferromagnetic chain, *Annals of Physics* **16**, 407 (1961).

[42] P. Pfeuty, The one-dimensional Ising model with a transverse field, *Annals of Physics* **57**, 79 (1970).

[43] For simplicity, hereafter we set $J = 1$ as the energy scale and work in units of $\hbar = k_B = 1$.

[44] I. Peschel and V. Eisler, Reduced density matrices and entanglement entropy in free lattice models, *Journal of Physics A: Mathematical and Theoretical* **42**, 504003 (2009).

[45] A. Y. Kitaev, Unpaired majorana fermions in quantum wires, *Physics Uspekhi* **44**, 131 (2001).

[46] G. Vidal, J. I. Latorre, E. Rico, and A. Kitaev, Entanglement in quantum critical phenomena, *Physical Review Letters* **90**, 227902 (2003).

[47] J. I. Latorre, E. Rico, and G. Vidal, Ground state entanglement in quantum spin chains, *Quantum Information and Computation* **4**, 48 (2004).

[48] The Fisher-Hartwig conjecture was proven by Basor in Ref. [35, 36].

[49] P. Calabrese and F. H. L. Essler, Universal corrections to scaling for block entanglement in spin-1/2 XX chains, *Journal of Statistical Mechanics: Theory and Experiment* **2010**, P08029 (2010).

[50] DLMF, *NIST Digital Library of Mathematical Functions*, <http://dlmf.nist.gov/>, Release 1.1.6 of 2022-06-30, F. W. J. Olver, A. B. Olde Daalhuis, D. W. Lozier, B. I. Schneider, R. F. Boisvert, C. W. Clark, B. R. Miller, B. V. Saunders, H. S. Cohl, and M. A. McClain, eds.

[51] V. Eisler and I. Peschel, Entanglement in fermionic chains with interface defects, *Annalen der Physik* **522**, 679 (2010).

[52] V. Eisler and I. Peschel, On entanglement evolution across defects in critical chains, *EPL (Europhysics Letters)* **99**, 20001 (2012).

[53] P. Calabrese, M. Mintchev, and E. Vicari, Entanglement entropy of one-dimensional gases, *Phys. Rev. Lett.* **107**, 020601 (2011).

[54] P. Calabrese, M. Mintchev, and E. Vicari, The entanglement entropy of one-dimensional systems in continuous and homogeneous space, *Journal of Statistical Mechanics: Theory and Experiment* **2011**, P09028 (2011).

[55] P. Calabrese, M. Mintchev, and E. Vicari, Entanglement entropy of quantum wire junctions, *Journal of Physics A: Mathematical and Theoretical* **45**, 105206 (2012).

[56] E. Barouch, B. M. McCoy, and M. Dresden, Statistical Mechanics of the XY Model. I, *Phys. Rev. A* **2**, 1075 (1970).

[57] E. Barouch and B. M. McCoy, Statistical Mechanics of the XY Model. II. Spin-Correlation Functions, *Phys. Rev. A* **3**, 786 (1971).

[58] E. Barouch and B. M. McCoy, Statistical Mechanics of the XY Model. III, *Phys. Rev. A* **3**, 2137 (1971).

[59] F. Ares, J. G. Esteve, F. Falceto, and A. R. de Queiroz, Entanglement entropy in the long-range kitaev chain, *Phys. Rev. A* **97**, 062301 (2018).

[60] F. Ares, J. G. Esteve, F. Falceto, and Z. Zimborás, Sublogarithmic behaviour of the entanglement entropy in fermionic chains, *Journal of Statistical Mechanics: Theory and Experiment* **2019**, 93105 (2019).

[61] H. Widom, Asymptotic behavior of block Toeplitz matrices and determinants. II, *Advances in Mathematics* **21**, 1 (1976).

[62] E. L. Basor, A Localization Theorem for Toeplitz Determinants, *Indiana University Mathematics Journal* **28**, 975 (1979).

[63] P. Calabrese and J. Cardy, Entanglement entropy and conformal field theory, *Journal of Physics A: Mathematical and Theoretical* **42**, 504005 (2009).